

# Heavily Ga-doped Germanium-Tin Alloys by Molecular Beam Epitaxy

Wei Wang,<sup>1</sup> Vijay Richard D' Costa,<sup>1</sup> Sin Leng Lim,<sup>2</sup> Qian Zhou,<sup>1</sup> Eng Soon Tok,<sup>2</sup> and Yee-Chia Yeo.<sup>1,\*</sup>

<sup>1</sup> Department of Electrical and Computer Engineering, National University of Singapore (NUS), Singapore 117582.

<sup>2</sup> Department of Physics, National University of Singapore, Singapore 117551.

\*Phone: +65 6516-2298, Fax: +65 6779-1103, E-mail: yeo@ieee.org

## ABSTRACT

**BF<sub>2</sub><sup>+</sup> implantation with solid-phase epitaxial regrowth (SPER) is not suitable for realizing heavily p-type Ge<sub>1-x</sub>Sn<sub>x</sub> at high Sn content, due to the degraded crystalline quality. Heavily p-type Ge<sub>1-x</sub>Sn<sub>x</sub> alloys were realized by *in-situ* Ga doping, with an active doping concentration of up to 4.3×10<sup>20</sup> cm<sup>-3</sup>. The dependences of crystallinity and mobility on the active Ga concentrations were also investigated.**

## 1. INTRODUCTION

Germanium-tin (Ge<sub>1-x</sub>Sn<sub>x</sub>) is an attractive material candidate for future integrated devices, such as high mobility transistors, photodetectors (PDs), and lasers [1]-[3]. For successful device applications, low resistivity and low leakage Ge<sub>1-x</sub>Sn<sub>x</sub> p-n junctions are required. Boron is often used as a p-type dopant in Ge. Through solid-phase epitaxial regrowth (SPER), active levels of 2-5.7×10<sup>20</sup> cm<sup>-3</sup> were demonstrated [4]. We have reported that after BF<sub>2</sub><sup>+</sup> implantation, boron can be activated during SPER at 400 °C in Ge<sub>1-x</sub>Sn<sub>x</sub> [5]. However, the crystallinity of the Ge<sub>1-x</sub>Sn<sub>x</sub> was not investigated. Ga is another p-type dopant in Ge or Ge<sub>1-x</sub>Sn<sub>x</sub>. An active level of 5.5×10<sup>19</sup> cm<sup>-3</sup> was reported in Ge<sub>1-x</sub>Sn<sub>x</sub> by *in-situ* epitaxial growth [6].

In this work, we demonstrated that 500 °C SPER can recover the crystallinity of Ge<sub>0.975</sub>Sn<sub>0.025</sub> to the as-grown level. However, for Ge<sub>0.92</sub>Sn<sub>0.08</sub>, severe degradation of the crystallinity occurs after SPER. *In-situ* Ga doped Ge<sub>0.915</sub>Sn<sub>0.085</sub> alloys were grown by MBE, and an electrical activation level of 4.3×10<sup>20</sup> cm<sup>-3</sup> was achieved, which is close to the solubility limit of Ga in Ge.

## 2. BF<sub>2</sub><sup>+</sup> IMPLANTATION AND SPER

The Ge<sub>1-x</sub>Sn<sub>x</sub> alloys were grown at 170 °C by MBE. A BF<sub>2</sub><sup>+</sup> implant of 1×10<sup>15</sup> cm<sup>-2</sup> at 20 keV was carried out, followed by rapid thermal annealing at various temperatures. Fig. 1(a) shows that after annealing at 500 °C, the Ge<sub>0.975</sub>Sn<sub>0.025</sub> peak and related thickness fringes in XRD scan become similar to that of as-grown sample, indicating recovery of crystallinity. However, for the Ge<sub>0.92</sub>Sn<sub>0.08</sub> sample, a shoulder between Ge<sub>0.92</sub>Sn<sub>0.08</sub> and Ge peaks appears after 500 °C annealing, which may arise from Sn precipitation or surface segregation. These results suggest that SPER after implantation is not suitable for realization of high-quality p-type region in Ge<sub>1-x</sub>Sn<sub>x</sub> with x > 0.08.

## 3. IN-SITU GA DOPED GESN BY MBE

*In-situ* Ga doped Ge<sub>0.915</sub>Sn<sub>0.085</sub> alloys were also grown by MBE on n-type Ge(100) substrate. During growth, the temperatures of Ge and Sn cells were fixed, and that of Ga cell was tuned to achieve various Ga concentrations. 4 samples were grown with Ga cell temperature ranging from 540 to 820 °C. Fig. 2 shows the resistivity of Ge<sub>0.915</sub>Sn<sub>0.085</sub> samples with various Ga concentrations by micro four-point probe measurements. Infrared spectroscopic ellipsometry was then used to obtain the active Ga concentration and mobility separately. Ellipsometric angles Ψ and Δ were acquired at two angles of incidence (65° and 75°) from 0.06 to 0.6 eV. The infrared response of a p-type Ge<sub>1-x</sub>Sn<sub>x</sub> alloy is dominated by free carrier response. Fig. 3 shows the fits (Ref. [7]) to Ψ and Δ. The free carrier absorption was described by a Drude oscillator from which active Ga concentration was extracted. The infrared dielectric function for various p-doped Ge<sub>0.915</sub>Sn<sub>0.085</sub>

alloys is shown in Figs. 4(a) and 4(b). As indicated by ε<sub>2</sub>, the free-carrier absorption increases with increasing Ga cell temperature, with the active Ga concentration ranging from ~10<sup>18</sup> to 4.3×10<sup>20</sup> cm<sup>-3</sup>.

Fig. 5 shows the electrical resistivity of p-type Ge<sub>1-x</sub>Sn<sub>x</sub> alloys as a function of doping concentration. The results for bulk Ge, *in-situ* boron-doped Ge<sub>1-x</sub>Sn<sub>x</sub> by CVD [7,8], and *in-situ* Ga-doped Ge<sub>1-x</sub>Sn<sub>x</sub> by MBE [6] are also included. It is observed that the resistivity values of Ge<sub>1-x</sub>Sn<sub>x</sub> samples follow the trend, but are slightly higher than those of p-type Ge bulk materials. These results suggest degradation of mobility in p-type Ge<sub>1-x</sub>Sn<sub>x</sub> alloys, which is likely due to alloy scattering in the Ge-Sn system. With the p-type concentration increased to ~10<sup>20</sup> cm<sup>-3</sup> or above, the ionized impurity scattering becomes severe, and the resistivity of Ge<sub>1-x</sub>Sn<sub>x</sub> alloys is similar to that of Ge bulk materials.

Fig. 6 shows the (004) XRD scans of Ge<sub>0.915</sub>Sn<sub>0.085</sub> samples with various active Ga concentrations. Well-defined Ge<sub>0.915</sub>Sn<sub>0.085</sub> peak and clear thickness fringes can be observed with the active Ga concentration up to 1.6×10<sup>20</sup> cm<sup>-3</sup> (740 °C). Fig. 7(a) shows the cross-sectional TEM image of Ge<sub>0.915</sub>Sn<sub>0.085</sub> sample with active Ga concentration of 1.6×10<sup>20</sup> cm<sup>-3</sup>. High resolution TEM images [Figs. 7(b) and 7(c)] depict smooth surface and good Ge<sub>0.915</sub>Sn<sub>0.085</sub>/Ge interface. No obvious defect can be observed. With the active Ga concentration increasing to 4.3×10<sup>20</sup> cm<sup>-3</sup> (820 °C), the Ge<sub>1-x</sub>Sn<sub>x</sub> peak shifts toward the Ge peak (Fig. 6), which indicated a reduction of Sn content. Fig. 8 shows the SIMS depth profiles of Ga and Sn with various active Ga concentrations. The Ga concentration in Fig. 8(a) was quantified by assuming that the Ge<sub>0.915</sub>Sn<sub>0.085</sub> sample with an active Ga concentration of 1.7×10<sup>19</sup> cm<sup>-3</sup> (640 °C) is fully electrically active. The Sn content in Fig. 8(b) was quantified by XRD. The depth profiles of Ga and Sn are uniform in Ge<sub>0.915</sub>Sn<sub>0.085</sub> layer with the active Ga concentration up to 1.6×10<sup>20</sup> cm<sup>-3</sup>. However, with the active Ga concentration increased to 4.3×10<sup>20</sup> cm<sup>-3</sup>, the Ga and Sn profiles become nonuniform, and both gradually increase toward the surface. These results suggest that when the incorporated Ga concentration exceeds the solid solubility limit, extra Ga atoms cannot be activated, and will lead to degradation of Ge<sub>1-x</sub>Sn<sub>x</sub> crystallinity.

## 4. CONCLUSION

We demonstrated that BF<sub>2</sub><sup>+</sup> implantation and SPER is not suitable for realizing heavily p-type Ge<sub>1-x</sub>Sn<sub>x</sub>, due to the degraded crystalline quality. Heavily p-type Ge<sub>1-x</sub>Sn<sub>x</sub> can be realized by *in-situ* Ga doping, with an active doping concentration of up to 4.3×10<sup>20</sup> cm<sup>-3</sup>. The dependences of crystallinity and mobility on the active Ga concentrations were also investigated.

**ACKNOWLEDGEMENT.** This work was supported by Singapore National Research Foundation through the Competitive Research Program (Grant No: NRF-CRP6-2010-4).

## References

- [1] P. Guo *et al.*, *JAP* 114, 044510, 2013.
- [2] Y. Dong *et al.*, *TED* 62, 128, 2015.
- [3] S. Wirth *et al.*, *Nature Photonics* 9, 88, 2015.
- [4] S. Mirabella *et al.*, *APL* 92, 251909, 2008.
- [5] G. Han *et al.*, *IWJT*, 106, 2012
- [6] Y. Shimura *et al.*, *Thin Solid Films* 520, 3206, 2012.
- [7] V. R. D'Costa *et al.*, *PRB* 80, 125209, 2009.
- [8] B. Vincent *et al.*, *APL* 99, 152103, 2011.

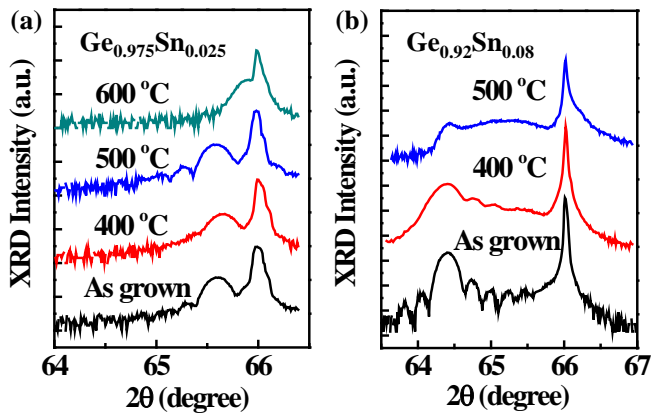


Fig. 1. XRD (004) curves of  $\text{BF}_2^+$  implanted (a)  $\text{Ge}_{0.975}\text{Sn}_{0.025}$  and (b)  $\text{Ge}_{0.92}\text{Sn}_{0.08}$  films after RTA at various temperatures for 5 minutes. For  $\text{Ge}_{0.92}\text{Sn}_{0.08}$  film, anneal cannot recover crystallinity to as-grown level.

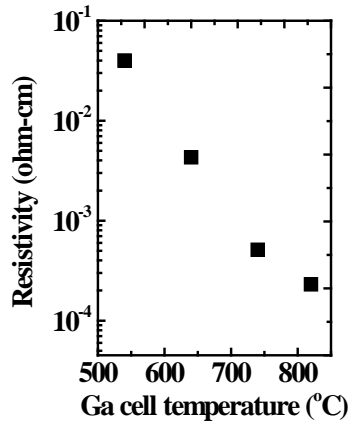


Fig. 2. The resistivity of  $\text{Ge}_{0.915}\text{Sn}_{0.085}$  films with various *in-situ* Ga doping concentration.

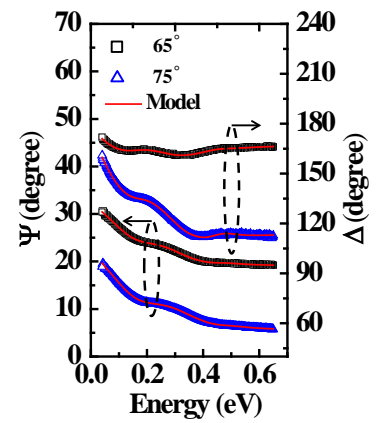


Fig. 3. Measured and fitted  $\Psi$  and  $\Delta$  from infrared ellipsometry for a  $\text{Ge}_{0.915}\text{Sn}_{0.085}$  film. An active Ga concentration of  $1.6 \times 10^{20} \text{ cm}^{-3}$  was obtained from the Drude model.

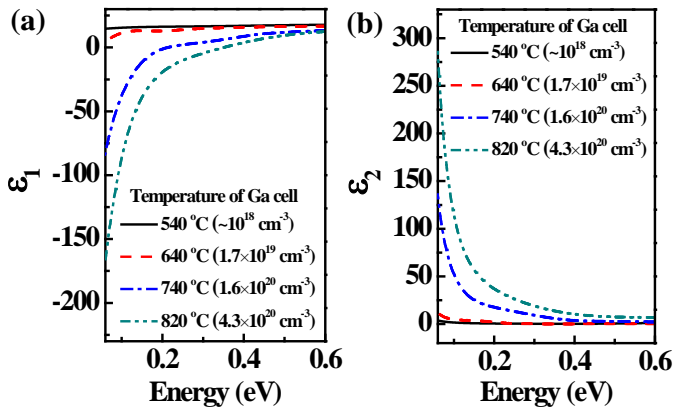


Fig. 4. (a) Real and (b) imaginary parts of infrared dielectric function of *p*-doped  $\text{Ge}_{0.915}\text{Sn}_{0.085}$  films. The curves reveal strong free-carrier response.

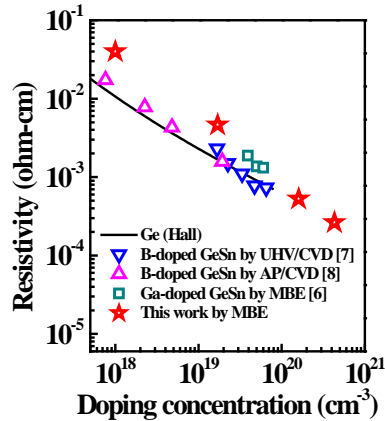


Fig. 5. Electrical resistivity of *p*-type  $\text{Ge}_{1-x}\text{Sn}_x$  alloys as a function of doping concentration.

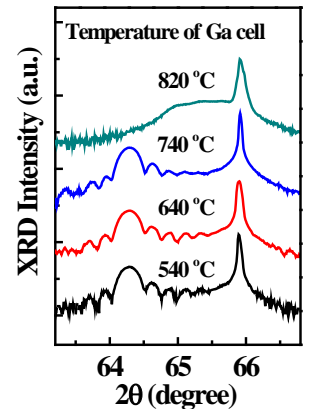


Fig. 6. XRD (004) curves of  $\text{Ge}_{0.915}\text{Sn}_{0.085}$  films with various *in-situ* Ga doping concentration.

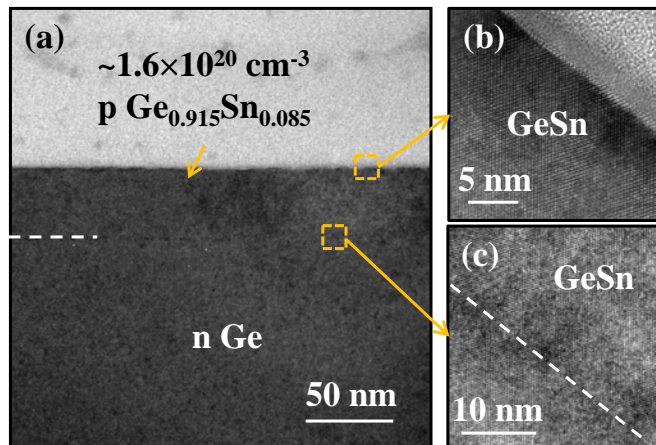


Fig. 7. (a) The cross-sectional TEM image of Ga-doped  $\text{Ge}_{0.915}\text{Sn}_{0.085}$  film with an active Ga concentration of  $1.6 \times 10^{20} \text{ cm}^{-3}$ . HRTEM image of (b) surface region and (c) interface region between  $\text{Ge}_{0.915}\text{Sn}_{0.085}$  and Ge.

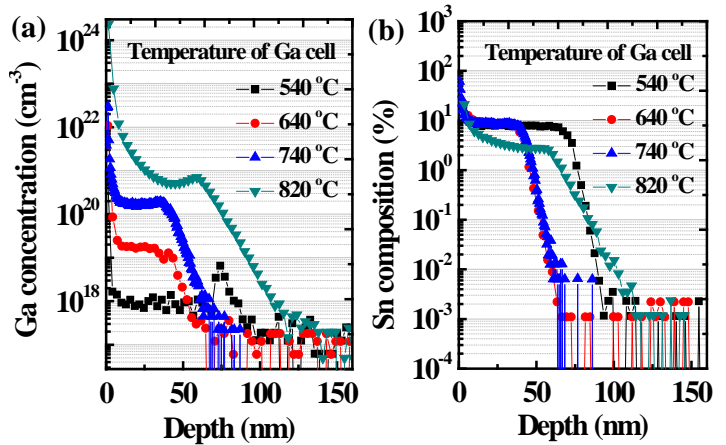


Fig. 8. SIMS depth profiles of (a) Ga and (b) Sn for  $\text{Ge}_{0.915}\text{Sn}_{0.085}$  films with various *in-situ* Ga doping concentration, which was tuned by the temperature of Ga cell during growth.